Bridging Nanogap Electrodes by In Situ Electropolymerization of a Bis(terthiophenylphenanthroline)ruthenium Complex

Koiti Araki,*[a, b, d] Hiroaki Endo,[a, b] Gou Masuda,[c] and Takuji Ogawa*[a, b]

Abstract: A novel complex containing a 3,8-bis[terthiophenyl-(1,10-phenanthroline)] ligand coordinated to $[Ru(bpy)_2]$ was synthesized and characterized by electrochemical and spectroscopic techniques. The complex was shown to be a suitable starting material for the electrodeposition of functionalized molecular wires between nanogap electrodes to generate stable molecular nanodevices. Temperature-dependent nonlinear *I–V* curves were obtained at 80–300 K. The material can also be deposited on indium tin oxide (ITO) to form compact electrochromic films at surface concentrations lower than $\approx 1 \times 10^{-8}$ mol cm^2; however, a more loosely bond fibrous form is preferentially deposited at higher surface concentrations.

Keywords: conducting materials · electrochemistry · N ligands · nanogap devices · ruthenium

Introduction

The development of molecular devices requires the preparation of functional materials with suitable properties.[1] Molecular wires based on, for example, phenylacetylene, thiophenylacetylene, and phenylenevinylene frameworks have been proposed and realized;[2] however, the preparation of long unidimensional conducting molecules is still hampered by synthetic difficulties. Also, little has been reported on the measurement of molecular conduction properties,[3–5] and the majority of the devices were prepared by means of break junction or electrical migration techniques. Such devices are very difficult to fabricate, and they seem to be too fragile for practical applications. To overcome these difficulties, we started to pursue the possibility of using arrays of molecules and nanoparticles for that purpose. In previous work, we showed that stable arrays of gold nanoparticles can be easily obtained with 1,10-decanedithiol bridging units.[6] This material exhibits semiconductor-like properties with characteristic sigmoidal-shaped *I–V* curves and a linear $\log I$ versus $1/T$ relationship when attached to gold microelectrodes, in contrast with the bulk material that showed ohmic behavior. The difference was attributed to mesoscopic effects, and was explained by means of the Coulomb blockade theory. Herein, we describe the synthesis and characterization of new bis(thienyl)-1,10-phenanthrolines coordinated to a $[Ru(bpy)_2]$ group (Scheme 1 and Scheme 2). The bis(terthienyl) derivative is electropolymerizable and was used to connect nanogap electrodes to generate stable molecular devices that exhibit temperature-dependent nonlinear *I–V* curves.

[a] Dr. K. Araki, H. Endo, Prof. Dr. T. Ogawa
Research Center for Molecular Nanoscience
Institute for Molecular Science
Okazaki National Research Institutes
Nishigo-Naka 38, Myodaiji-cho, Okazaki, Aichi, 444-8585 (Japan)
E-mail: koiaraki@iq.usp.br
ogawat@ims.ac.jp

[b] Dr. K. Araki, H. Endo, Prof. Dr. T. Ogawa
Japan and Core Research for Evolutional Science and Technology (CREST) of Japan Science and Technology Agency (JST)
Hon-machi 4-1-8, Kawaguchi, Saitama, 332-0012 (Japan)
Fax: (+81) 564-59-5635

[c] G. Masuda
Department of Chemistry, Faculty of Science
Ehime University
Bunkyo-cho 2–5, Matsuyama, Ehime, 790-8577 (Japan)

[d] Dr. K. Araki
Instituto de Química - Universidade de São Paulo
Av. Prof. Lineu Prestes, 748 - Butantã
05508–900 São Paulo (Brazil)

Results and Discussion

π-Conjugated conducting polymers and oligomers containing electrochemically and photochemically active transition-metal complexes, such as $[Ru(bpy)_3]$, are of great interest as materials for molecular devices.[7,8] In particular, linear wires with extended π systems interacting with metal complexes are potential candidates for the preparation of functional single-molecule devices. The molecular conduction is believed to occur by tunneling and should be proportional to the negative exponential of the square root of the energy gap and the chain length.[5] Both parameters can be varied;

 DOI: 10.1002/chem.200400063

however, the energy gap is particularly sensitive to the degree of π delocalization in the molecular wire.[9–11] The metal complexes were assumed to impart some functionality, for example, by acting as charge-trapping sites in single-electron transistors[3] or electron hopping and photoactive sites. Finally, a simple method for deposition of a molecular material directly in place to afford stable junctions was pursued. Electropolymerization seemed to satisfy these requirements, and compound **11** (Scheme 2) was chosen as prototype monomer. Complexes **3** and **13** were utilized in the characterization process.

Synthesis: The phenanthroline derivatives were obtained after a multistep synthesis involving Pd- or Ni-catalyzed cross-coupling to 3,8-dibromo-1,10-phenanthroline,[12] which was obtained by bromination of commercially available 1,10-phenanthroline monohydrate in the presence of S_2Cl_2. Compound **2** was obtained by Ni-catalyzed cross-coupling of dibromophenanthroline with the appropriate Grignard reagent (Scheme 1).

A similar strategy was used to prepare the terthienyl-substituted phenanthroline derivatives. Initially, the synthesis of the unsubstituted bis(terthienyl)phenanthroline was attempted by the Ni-catalyzed reaction of the Grignard reagent of 5″-bromo-2,2′:5′,2″-terthiophene with **1**; however, the reaction was hindered by the low solubility of this reagent. To overcome this drawback, two *n*-butyl radicals were introduced into the 3,4-positions of the middle thiophene ring (Scheme 2). This strategy was successful, and the desired phenanthroline derivative **10** was obtained in 40% yield. This was subsequently converted to the corresponding ruthenium polypyridine complex **11** by reaction with $[Ru(bpy)_2(OH_2)_2](NO_3)_2$ in DMF. Compound **10** was also allowed to react with Br_2 and KSCN to give the thiocyano derivative **12**, and subsequently converted to the ruthenium complex **13**, as described above. All steps gave reasonable-to-high yields making the strategy convenient for the preparation of these functionalized thiophene derivatives. The NMR and mass spectra and the elemental analysis of the compounds were consistent with the structures shown in Scheme 1 and Scheme 2.

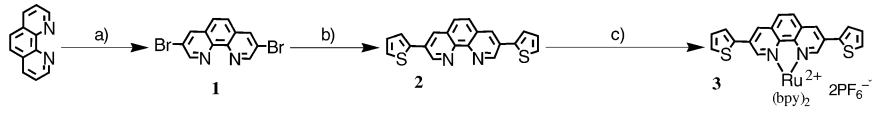

Scheme 1. Procedure for the preparation of complex **3** from phenanthroline. a) Br_2, S_2Cl_2, *n*-BuCl, py, 62%; b) [Ni(Cl_2(dppp)], THF, 94%; c) 1. $[Ru(bpy)_2(OH)_2]$/DMF, 2. NH_4PF_6, 80%.

UV/Vis spectra: The spectra of oligothiophenes are known to exhibit a band at around 245 nm, and a second band, whose energy is dependent on the chain length, at higher

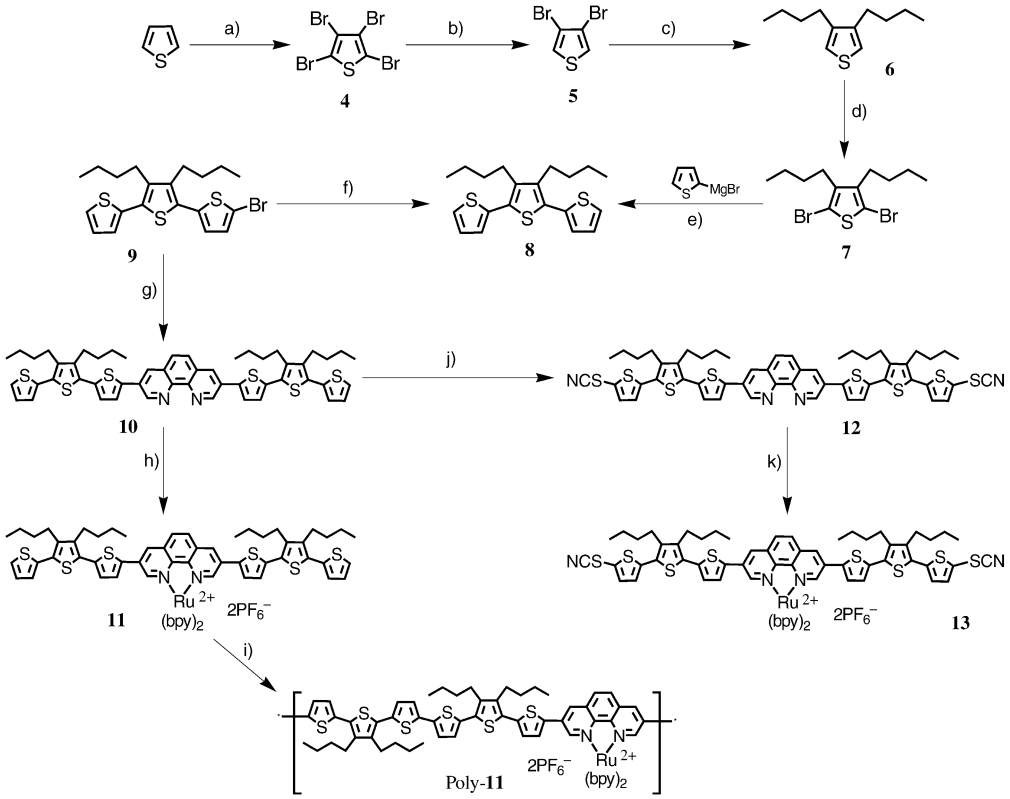

Scheme 2. Scheme for the preparation of complexes **11**, **13**, and poly-**11**. a) Br_2, $CHCl_3$, 90%; b) Zn, AcOH, H_2O, 86%; c) [$NiCl_2$(dppp)], Et_2O, 85%, $CH_3(CH_2)_3MgBr$; d) Br_2, AcOH, $CHCl_3$, 87%; e) [$NiCl_2$(dppp)], Et_2O, 84%; f) AcOH/$CHCl_3$, NBS, 61%; g) 1. Mg/THF, 2. [$NiCl_2$(dppp)]/THF, 40%; h) 1. $[Ru(bpy)_2(OH_2)_2]$/DMF, 2. NH_4PF_6, 71%; i) electropolymerization in MeCN/$TBAClO_4$ 0.1 M; j) Br_2, KSCN, MeOH, $CHCl_3$, 94%; k) 1. $[Ru(bpy)_2(OH_2)_2]$/DMF, 2. NH_4PF_6, 84%. dppp = 1,3-bis(diphenylphosphanyl)propane; NBS = *N*-bromosuccinimide.

wavelengths. The first one is assigned to an intraring π–π* transition, and the second to a π–π* transition of the conjugated π system. This band is strongly influenced by the presence of electron-accepting groups, such as pyridine derivatives, directly bonded to the thiophene chain. Accordingly, the red shift was attributed to contributions from donor–acceptor charge-transfer interactions by Yamamoto et al.[13,14] Nevertheless, relatively modest shifts were observed in oligothiophene-bridged 2,2′-bpy derivatives by Pappenfus et al., who found a linear correlation between the energy of that transition and the number of conjugated rings when the pyridine rings were considered.[15] Accordingly, the red shift was assigned to the participation of the bpy rings in the extended π system of the oligothiophene chain, because the π–π* transition is known to be shifted to lower energies as the number of thiophene rings is increased.[16,17] The 3,8-bis-(thiophene)-1,10-phenanthroline derivatives **2**, **10**, and **12** also belong to such a class of compounds and should exhibit a similar behavior. The lowest energy band appeared at 340 nm in the spectrum of compound **2** in DMF. It is shifted to 419 and 422 nm (Figure 1) in compounds **12** and **10**, respectively. These wavelengths are comparable to those of other analogous oligothiophene derivatives.[7,9,15]

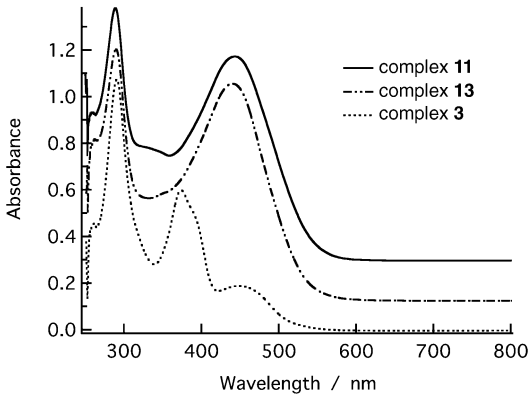

Figure 1. UV/Vis spectra of complexes **3**, **11**, and **13** in DMF.

The coordination of $[Ru(bpy)_2]$ should strongly influence the electronic properties of the phenanthroline ring, which may affect the degree of π conjugation in the thiophene backbone. Complex **3** exhibits the ruthenium complex bands at 290 and 454 nm, respectively, assigned to the characteristic bpy π–π* transition and $Ru^{II}(d\pi)$-to-bpy(pπ*) and -phen(pπ*) charge-transfer transitions. The band at 372 nm can be attributed to the thiophene π–π* transition. The red shift reflects the effect of the ruthenium complex coordination on the conjugated π system. A weak band, assigned to a d–d transition, is also expected at about 350 nm; however, it should be hidden under the more intense π–π* bands nearby. Only one intense and broad band is visible at about 442 nm in the case of the complexes **11** and **13**. This envelope contains the terthiophene π–π* and ruthenium complex charge-transfer transitions, as can be inferred by its higher molar absorptivity ($7.8\times10^4\,M^{-1}cm^{-1}$) compared to a conventional MLCT band in similar compounds ($\approx1.5\times10^4\,M^{-1}\,cm^{-1}$).[18] This means that the electronic absorption spectra can be satisfactorily explained if the energy levels are considered to be essentially localized in the thiophene backbone and the ruthenium polypyridine complex.

Electrochemistry: The electrochemical behavior of the ruthenium complexes **3**, **11**, and **13** was examined by cyclic voltammetry and is summarized in Table 1. The voltammograms in DMF were generally more reversible than in acetonitrile where adsorption occurred more promptly, particularly because of their much lower solubilities in the last solvent. Compound **3** exhibited five reversible monoelectronic processes at 1.31, −1.18, −1.45, −1.68 and −1.94 V versus SCE, in DMF and acetonitrile solution (Figure 2). The reversible redox couple at 1.31 V is readily assigned to the $Ru^{III/}Ru^{II}$ process. No other oxidation reaction could be found up to 2 V, in analogy with the results obtained by Pappenfus et al. for the binuclear $[Ru(bipy)_3]$ complex bridged by a thienyl ring.[15]

The assignment of the reduction processes is more complicated. A comparison of the potentials in Table 1 indicated that the first ligand-centered reduction of complex **3** is shifted to more positive potentials by about 200 mV than those of the $[Ru(bpy)_3]$ and $[Ru(phen)_3]$ complexes. However, even more pronounced shifts have been reported for analogous ruthenium complexes with a bipyridine ligand bonded to thienyl and bisthienyl radicals at the 5,5′-positions.[11,19,20] Consequently, the reduction process at −1.18 V was attributed to the monoelectronic reduction of the phenanthroline ligand. The following processes at −1.45 and −1.68 V were then assigned to the successive monoelectronic reductions of

Table 1. Redox potentials (V versus SCE) of the ruthenium complexes in DMF and acetonitrile solutions. The $E_{1/2}$ values were estimated as the average of the cathodic and anodic peak potentials. The potentials were corrected considering the potential of the Fc/Fc^+ process as being 0.40 V versus SCE.

Complex[a]	$E_{1/2}$(ox)[b]	L/L^{-}[b]	$bpy_1^{0/-}$	$bpy_2^{0/-}$[b]	L^{-}/L^{2-}
$[Ru(bpy)_3]$[15,19,26]	1.26 (Ru^{III}/Ru^{II})	−1.34 ($bpy_1^{0/-}$)	−1.52	−1.78	
$[Ru(bpy)_2(phen)]$[26]	1.26	−1.36	−1.54	−1.79	
$[Ru(bpy)_2(tpbpy)]$[c][19]	1.54	−1.02	−1.34		
$[Ru(bpy)_2(btbpy)]$[c][11]		−1.10	−1.44	−1.63	
$[Ru(bpy)_2(\mathbf{2})]$[c]	1.32	−1.17	−1.44	−1.67	−1.97
$[Ru(bpy)_2(\mathbf{2})]$[d]	1.22	−1.18	−1.45	−1.68	−2.03
$[Ru(bpy)_2(\mathbf{10})]$[d]	1.06[ap], 1.24[ap]	−1.13	−1.44	−1.64	−1.82
$[Ru(bpy)_2(\mathbf{12})]$[d]	1.22[ap]	−1.15	−1.44	−1.66	−1.88
P4–Ru[c][19]	0.94, 1.10, 1.37(Ru^{III}/Ru^{II})	−1.02	−1.30		
P6–Ru[c][19]	0.79, 0.95, 1.31(Ru^{III}/Ru^{II})	−1.02	−1.33		
Poly-$[Ru(bpy)_2(\mathbf{10})]$[c]	0.85, 1.02, 1.36(Ru^{III}/Ru^{II})	−1.13[cp]	−1.50[cp]	−1.84[cp]	not observed

[a] tpbpy = 4,4′-bis(3-dioctylthienyl)-2,2′-bipyridine, btbpy = 4,4′-bithienyl-2,2′-bipyridine, P4-Ru = poly-{$(bpy)_2$Ru(1,10-phen-5,5′-bis(3,3′,3″,3‴-tetraoctyl-2,2′:5′,2″:5″,2‴:5‴,2⁗-quaterthiophene), P6–Ru = analogous to P4–Ru, but with hexathienyl radicals. [b] ap = anodic peak potential, cp = cathodic peak potential. [c] In acetonitrile. [d] In DMF.

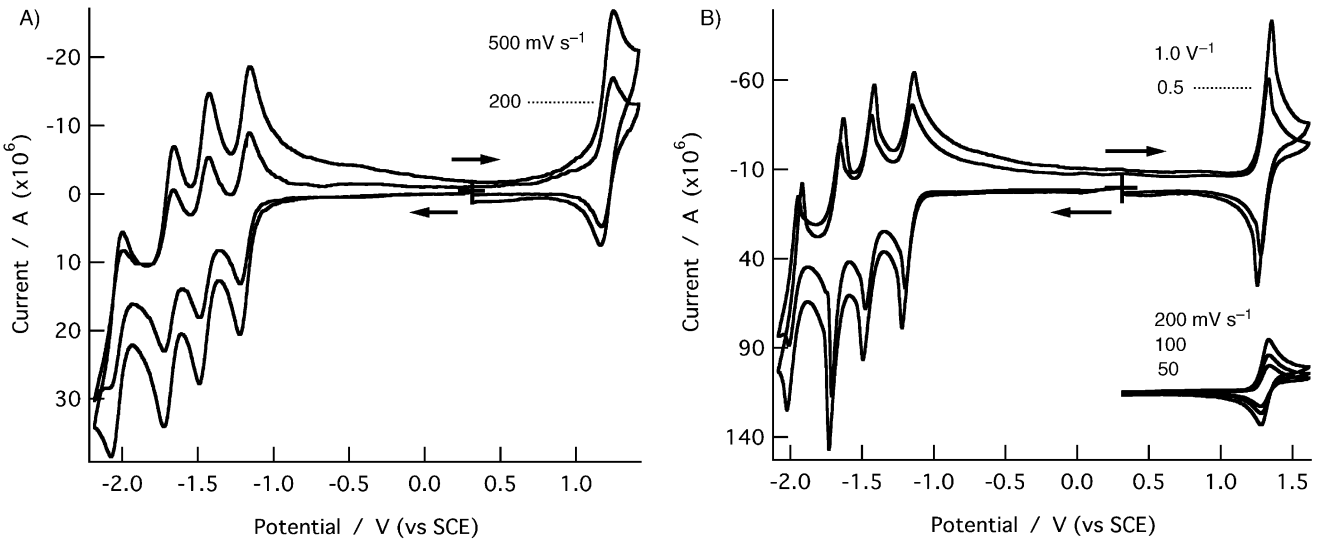

Figure 2. Cyclic voltammograms of complex **3** in A) 2.5 mM DMF and B) 3.5 mM acetonitrile, containing 0.1 M of $TBAClO_4$. The voltammograms in the 0.3–1.6 V range were shifted by 115 μA to facilitate visualization. The scan rates are indicated in the figure.

each of the bpy ligands. As expected, these redox potentials remained more or less constant for all three complexes. Generally, no other wave can be found next to this set of waves, but a fourth reversible process was observed for all ruthenium complexes at about −1.94 V. Similar results were reported for analogous heteroleptic ruthenium complexes with diimine ligands carrying electron-withdrawing groups or having larger aromatic structures.[21] Accordingly, it was tentatively assigned to the second monoelectronic reduction of the substituted phenanthroline ligand. The anodic counterpeak of this last process decreased as the scan rate diminished, exhibiting a typical EC mechanism profile, probably attributable to the reaction of that reduced species with some trace impurities present in the solvent. All processes were diffusion-controlled, as attested by the linear relationship between the current and the square root of the scan rate (not shown). The electrochemical behavior of complex **3** in MeCN is similar to that in DMF, except that sharp adsorption peaks are superimposed on the diffusion-controlled waves, as can be seen in Figure 2B. This effect is more pronounced for the cathodic peak at −1.7 V, whose relative intensity increases dramatically at low scan rates. But when the measurements were limited to the 0.3–1.6 V range, a typical diffusion-controlled reversible behavior was observed for the $Ru^{III/}Ru^{II}$ process at 1.32 V (Figure 2B).

The electrochemical behavior of the ruthenium complexes **11** and **13** was slightly different from that described above for compound **3**. The difference is associated with the electrochemical activity of the terthiophene moiety as well as the tendency of the oxidized species, with free terminal α-positions, to polymerize.[17] The comparative electrochemical study was carried out only in DMF because of the low solubility of compound **13** in acetonitrile.

The reduction of compound **11** in the 0 to −2.2 V range led to four reversible processes at −1.13, −1.44, −1.64, and −1.82 V versus SCE (Figure 3A), which were assigned in the same way as for compound **3**. The CVs of compound **13** were similar to that described above (Figure 3B); however, the first cathodic peak was slightly enhanced, probably attributable to an EC mechanism involving the reduction of the thiocyano radical. This assumption is confirmed by the appearance of an irreversible oxidation wave at −80 mV, which is absent in the voltammograms of compound **11** (Figure 3). This chemical process did not change the voltammetric behavior of the three subsequent processes (monoelectronic and reversible), nor the profile of the anodic wave at −1.15 V, corresponding to its counterpeak. The oxidation profile was irreversible for both complexes, showing a couple of intense peaks at 1.0 and 1.2 V for compound **11**, a peak at 1.2 V for **13**, and a reduction peak at about −0.6 V (not shown). This is consistent with the irreversible oxidation of polythiophenepyridines[13] and oligothiophenes bonded to ferrocene.[9] However, no associated reduction process was observed for the $Ru^{III/}Ru^{II}$ reaction regardless of its reversible character. This strongly suggests that the Ru^{III} species was being rapidly reduced to Ru^{II} by the terthienyl radicals. Interestingly, the Pt electrode remained clean in the case of compound **11**, but a white solid was deposited in the case of compound **13**. Clearly, this is a reaction by-product and no attempt was made to characterize it further.

Preparation and properties of the polymer film: The electrochemical behavior of compound **11** in acetonitrile contrasts with that in DMF solution. In this case, a pattern typically found for the deposition of an electrochemically active material on the electrode surface was observed (Figure 4A). This electropolymerization process leads to the formation of linear hexathiophene chains bridged by phenanthroline[Ru(bipy)$_2$] units through the 3,8-positions. The details of the electropolymerization process and its electrochemical and optical properties are described below.

Two reversible processes were found at −1.12 and −1.34 V when the potentials were scanned from 0 to −1.6 V. Nevertheless, the anodic wave of the second process is more intense and bell-shaped, as can be seen in the first scan

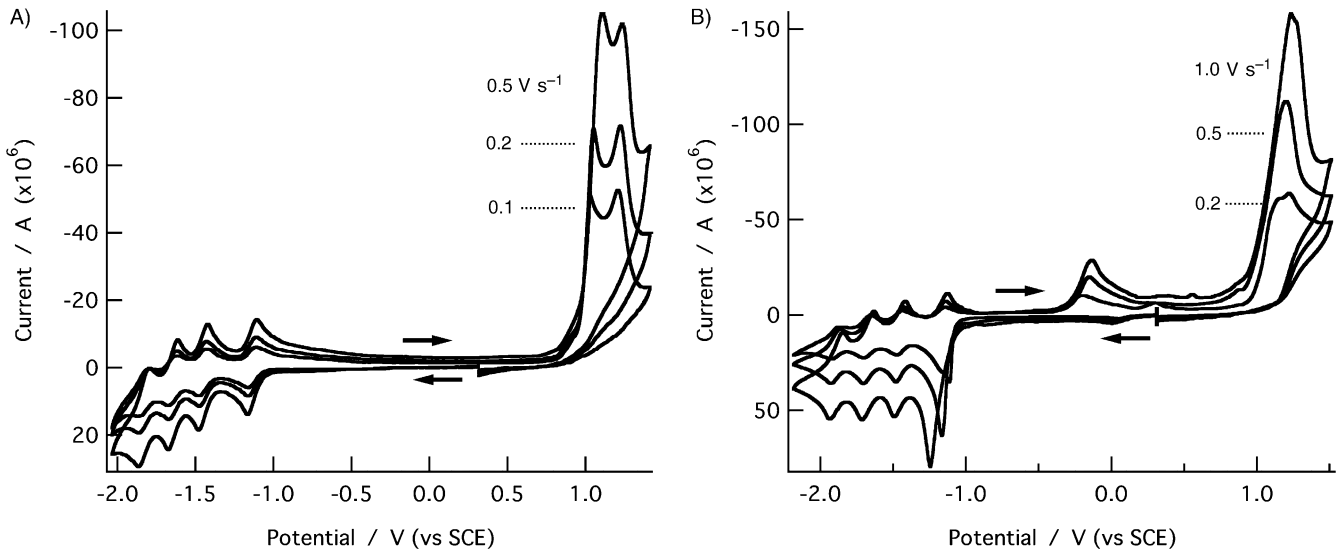

Figure 3. Cyclic voltammograms of A) 2.1 mM **11** and B) 2.0 mM **13** in a DMF solution containing 0.1 M $TBAClO_4$ with a Pt electrode. The scan rates are indicated in the figure.

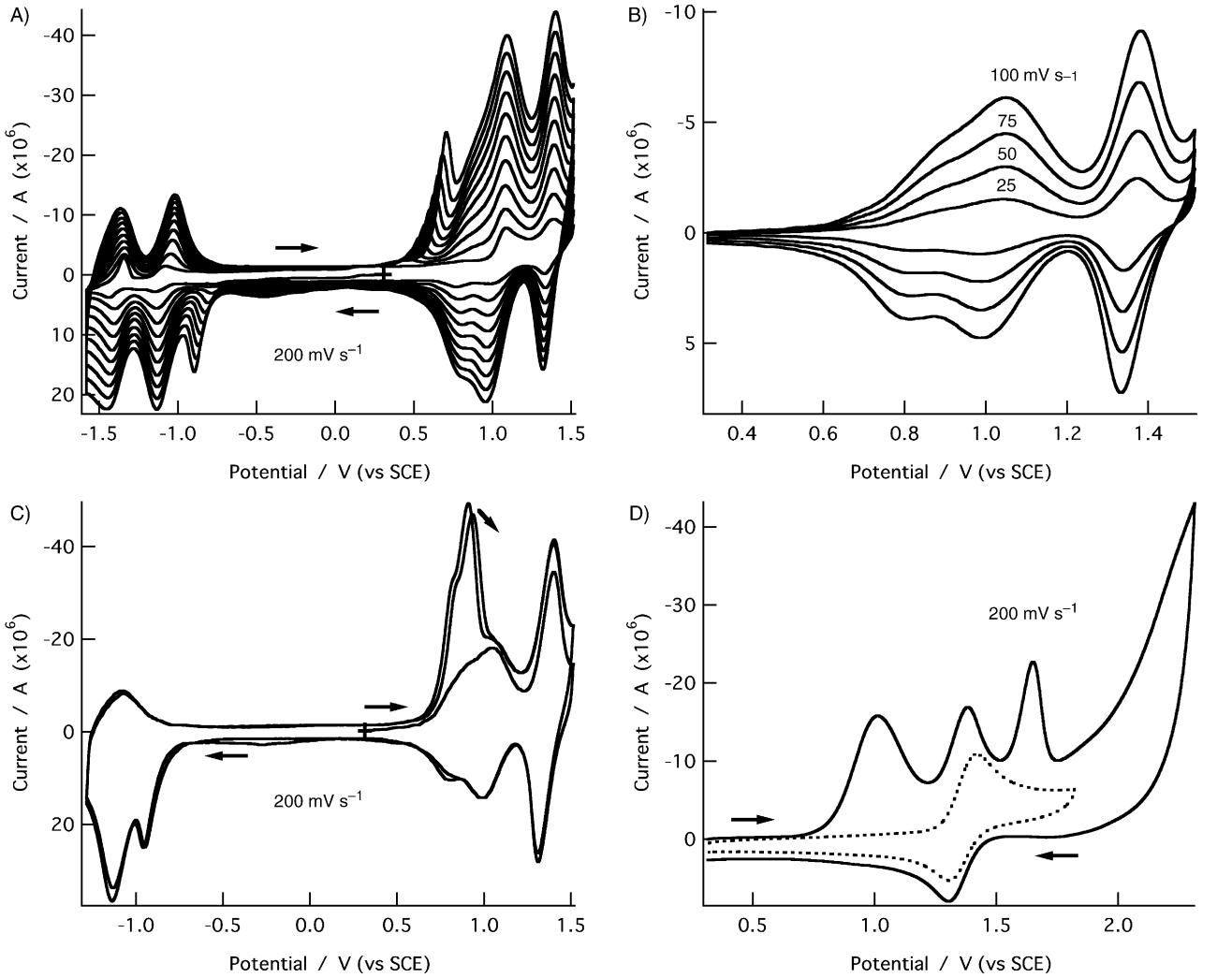

Figure 4. A) 10 successive cyclic voltammograms of a saturated solution of compound **11** from −1.6 to 1.5 V, 0.1 M $TBAClO_4$, Pt electrode. B) Cyclic voltammograms of an electrode modified with poly-**11** ($\Gamma = 1\times10^{-8}$ mol cm^{-2}) at different scan rates. C) Two successive scans from −1.3 to 1.5 V with the modified electrode obtained in (A) after scanning from 0.3–1.5 V. D) Cyclic voltammogram of poly-**11** in the 0.3–2.3 V range (——) followed by a scan in the 0.3–1.8 V range (-----). All experiments were carried out in a 0.1 M $TBAClO_4$ solution prepared with anhydrous acetonitrile.

trace. Accordingly, the doubly reduced species was adsorbing, and a relatively intense cathodic wave was found at about −1.8 V, when the potentials were scanned up to −2.0 V. The two most negative redox processes were irreversible, and a broadened anodic wave was found at −1.7 V (not shown). On the positive side, an irreversible and a reversible wave were found at E_{ap} = 1.08 and 1.38 V and assigned to the monoelectronic oxidation of ligand **10** and to the $Ru^{III/}Ru^{II}$ process, respectively. In the reverse scan, the wave attributed to the reoxidation of the Ru^{III} sites was followed by a couple of waves at E_{cp} = 0.96 and 0.77 V, attributed to the reduction of the electrochemically generated oxidized poly-**11** (Figure 4A). This contrasts with the electrochemical behavior in DMF solution described above.

In the subsequent scans, the waves related to the reduction of the phenanthroline and bipyridine ligands were built up, as well as an irreversible cathodic peak at about −0.86 V, which shifted to more negative potentials as a function of the number of scans. It should be noted, however, that the reoxidation waves at −1.37 and −1.02 V were smaller than the corresponding reduction waves, and they stopped growing after about seven cycles, while the other peaks continue to rise. This indicates that the reoxidation reactions were incomplete at those potentials, and is in fact occurring at 0.6 V. This irreversible peak is absent when the eletropolymerization process is carried out in the 0.0–1.5 V range and, after few cycles, the successive voltammograms became similar to that shown in Figure 4B. The low reversibility of these reoxidation processes in the polymer film becomes evident in the CV of a modified Pt electrode (−1.3 to 1.5 V range) in neat electrolyte solution (Figure 4C). In this case, a sharp anodic wave appeared superimposed on the reversible polymer waves at 0.8 V, but only after the reduction of the polymer at about −1.2 V. The following successive voltammograms (up to 10 scans) remained almost unchanged, except for a shift and decrease of that peak. However, the film is rapidly destroyed if the potentials are scanned up to −2.0 V. Also, the hexathiophene chain becomes electrochemically inactive when oxidized at 1.65 V, as shown in Figure 4D. Only the hexathienyl segments were affected by the process, as confirmed by the presence of the $Ru^{III/}Ru^{II}$ wave in the subsequent voltamograms. Consequently, only the processes in the 0.3–1.5 V range are electrochemically reversible, and their respective currents are directly proportional to the scan rate (Figure 4B).

The hexathiophene/ruthenium ion ratio in the polymer is 1:1, and the charge consumed for the oxidation of the hexathienyl segments is about twice as large. Consequently, the two broad waves that precede the $Ru^{III/}Ru^{II}$ wave can be assigned to two successive monoelectronic oxidation processes. Accordingly, the hexathiophene moiety is oxidized to the radical cation at 0.85 V and to the dication at 1.02 V, as confirmed by spectroelectrochemistry (Figure 5). Zhu et al. have shown that the electronic properties of the bpy ligand are dependent on the substitution position by the thienyl radicals.[9,15] The 4,4′-substituted bpy (equivalent to 3,8-substituted phen) was found to favor the delocalization along the chain to the detriment of the electronic coupling to the metal center. The same kind of effect may be responsible

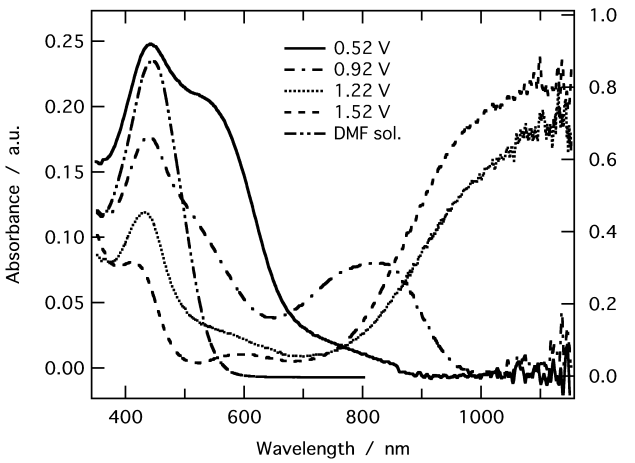

Figure 5. Spectroelectrochemistry of poly-**11** on ITO-glass in acetonitrile containing 0.1 M $TBAClO_4$. The spectra of the starting polymer $Ru^{II}HT^{0}$ (0.52 V), the hexathienyl radical cation $Ru^{II}HT^{+}$ (0.92 V), the dication $Ru^{II}HT^{2+}$ (1.22 V), and the $Ru^{III}HT^{2+}$ (1.52 V) species are shown. The spectrum of complex **11** in DMF solution was included for comparison. HT = hexathienyl radical.

for the broadening of the respective voltammetric waves in our complex; however, the contribution of some nonhomogeneity in the local microenvironment cannot be ruled out.

The electropolymerization reaction should lead to linear chains containing many ruthenium complexes bridged by hexathienyl segments. Despite the strong π delocalization in the conjugated backbone, bridging oligothiophenes[9,15] were shown to weakly couple transition-metal sites, even when two ruthenium bis(bipyridine) or terpyridine[22] complexes are connected by a single ring. Similar behavior has also been observed for large highly conjugated macrocycles, such as porphyrins,[23] but a strong coupling was reported for small heterocyclic ligands, such as pyrazines and benzotriazole.[24] In this case, the electronic states of the binuclear complexes are highly mixed, and the redox processes involving the metal sites are no longer degenerate. In our case, only one sharp and bell-shaped pair of peaks, displaced by ≈30 mV, were found for the $Ru^{III/}Ru^{II}$ process. This means that the full-width at half-maximum (FWHM = 115 mV at 100 mV s^{-1}) is close to the theoretical value of 90 mV, and that there is almost no interaction between the electrochemically active sites. Also, the chemical environment around the ruthenium sites should be very similar. The pattern described above is valid for thin films, such that much broader peaks separated further apart were found at higher surface concentrations. This effect is probably caused by impedances associated with the formation of a less firmly bound fibrous material, as confirmed by SEM microscopy (Figure 6).

Poly-**11** films can be deposited on different substrates, such as glassy carbon, gold, and ITO; however, they are relatively fragile. The films deposited on ITO exhibited absorption bands spanning the visible region up to 650 nm, at 440 and 540 nm (Figure 5, ——). These bands can be assigned to the Ru^{II}-to-polypyridine and -hexathiophene π–π* transitions, which were red-shifted after electropolymerization and formation of longer oligothiophene segments. When the polymer film was oxidized at 0.92 V, a characteristic band

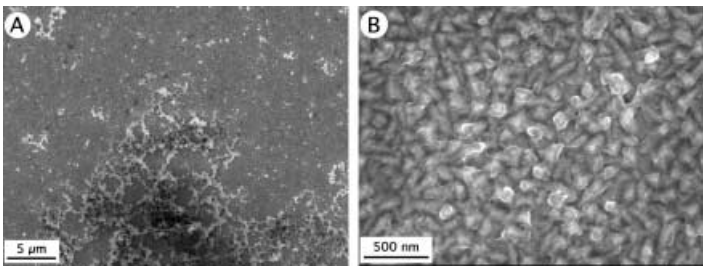

Figure 6. SEM microscopy images of ITO modified with poly-**11**, $\Gamma \approx 1 \times 10^{-8}$ mol cm^{-2}, showing A) the fibrous structures (×3300), and B) the ITO grains covered by a film of poly-**11** in an apparently clean region (× 45000).

appeared at 805 nm, and the absorbance at 540 nm decreased to approximately half its initial intensity. The second oxidation process at 1.22 V led to the appearance of a very broad band at 1100 nm and to the complete disappearance of the bands at 805 and 540 nm. These changes contrast with what is generally observed during the oxidation of analogous Ru^{II} complexes and are consistent with the formation of the hexathiophene radical cation and dication,[15,17] respectively. When the polymer was further oxidized at 1.52 V, the band characteristic of the dication at 1100 nm was significantly enhanced, and the absorbance in the 400 to 600 nm range diminished. This is attributed to the disappearance of the $Ru^{II}(d\pi)$-to-bpy($p\pi^*$) and -phen($p\pi^*$) charge-transfer transitions. The hexathiophene-to-ruthenium complex charge-transfer transition is absent in poly-**11**, in contrast with oligothiophenes bond to ferrocene,[7,9] because the Ru^{III} ion is an electron acceptor rather than a donor.

The morphology of poly-**11** deposited on ITO was analyzed by optical and scanning electron microscopy (SEM). The red-brown color of the polymer and the area covered by a fibrous material increased as a function of the surface concentration in the $\Gamma \approx 10^{-8}$ mol cm^{-2} range. An inspection of the modified surface by SEM with a similar magnification showed analogous structures (Figure 6A). However, the amount of poly-**11** on the surface seemed to be too low compared to the surface concentration. Accordingly, a closer inspection of the modified surface was carried out in comparison with the clean substrate. The result shown in Figure 6B revealed that the indium tin oxide (ITO) grains in apparently clean regions are in fact covered by a thin layer of poly-**11**, explaining the apparent inconsistency. This suggests that, at the beginning of the electropolymerization process, the polymer is obtained preferentially as a tight film on the surface of the grains. Nevertheless, a more loosely attached fibrous form seems to be favored as the surface concentration increases.

Current–voltage characteristics of poly-11: Electropolymerization was shown to be a suitable strategy for the preparation of poly-**11** directly between nanogap electrodes. This avoids complicated techniques to manipulate the molecular species for proper positioning and contact. Furthermore, the polymer chains may grow preferentially oriented along the electric field, forming a bunch of wires connecting the two electrodes. The HOMO and LUMO energies in different oxidation states were estimated from the electrochemistry and UV/Vis spectroscopy data, and compared with the Au Fermi level (Scheme 3).[7] It is easy to see that the HOMO of the neutral species is very close to the Au Fermi level, as

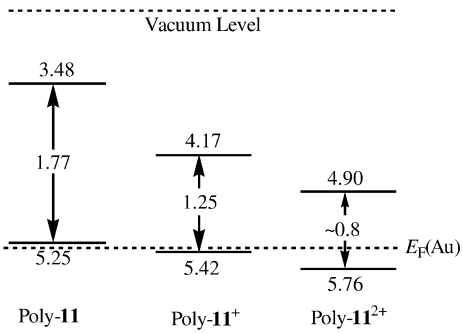

Scheme 3. Energy level [eV] diagram of poly-**11** in different oxidation states with reference to the vacuum level estimated from the electronic spectra and electrochemistry data; $E_F(Au) = 5.31$ eV.[27]

expected for a *p*-type material. The hole injection barrier is zero and the HOMO–LUMO gap, estimated from the absorption onset, is 1.77 eV. Temperature-dependent nonlinear *I–V* curves with similar profiles were obtained, as shown in Figure 7. The devices were stable enough to allow the collection of more than a hundred *I–V* curves as a function of the temperature without significant changes. They were generally symmetric, and the conductivity of the device decreased as the temperature was decreased from 300 to 80 K. Concomitantly, the "blockaded" region was widened and reached about 2.7 eV at 80 K, which is about 1 eV higher than the HOMO–LUMO gap. The strong temperature-dependence was successfully explained based on the thermionic and tunneling models, and is being published elsewhere.[25] Smaller energy gaps (1.25 and ~0.8 eV) are anticipated for poly-**11**$^+$ and poly-**11**$^{2+}$, respectively (Scheme 3).

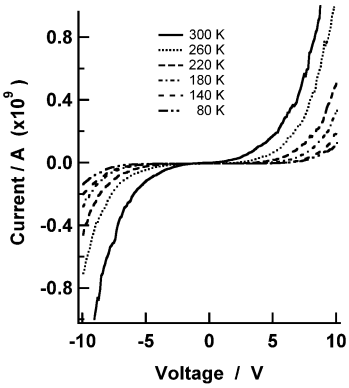

Figure 7. Typical temperature-dependent *I–V(T)* curves for poly-**11** on a gold nanoelectrode with a 15 nm gap at 80–300 K.

Conclusion

A new bis(terthienyl)-1,10-phenanthroline coordinated to $[Ru(bpy)_2]$ was synthesized and characterized by UV/Vis

spectroscopy and cyclic voltammetry. The electrochemistry of the three derivatives was consistent with that of analogous compounds: four reversible reduction processes were exhibited in the 0 to −2.2 V range. The voltammetric behavior was irreversible in the 0–1.5 V range for the terthienyl derivatives on account of its fast oxidation by the electrochemically generated Ru^{III} complexes. This reaction leads to electropolymerization and the build up of an electrochemically and electrochromically active material on the electrode surface from an acetonitrile solution. A tight film is generated on ITO at low surface concentrations, and a lose fibrous form is preferentially formed at higher concentrations. The monomer was shown to be a suitable starting material for the electrodeposition of functionalized molecular wires directly between gold electrodes separated by a nanometer-sized gap. Stable molecular devices exhibiting temperature-dependent nonlinear *I–V* curves were obtained in this way.

Experimental Section

All reagents and solvents were of analytical grade and used without further purification. The anhydrous solvents were drawn up into a syringe under a flow of dry N_2 gas and were directly transferred into the reaction flask to avoid contamination. The intermediates and products were characterized by elemental analysis and spectroscopic methods.

The UV/Vis spectra, in solution or as a polymeric film on ITO glass, were recorded with a Shimadzu UV-3150 double-beam spectrophotometer. The IR spectra were recorded in a Horiba FT-700 spectrophotometer. Cyclic voltammograms were registered with a BAS CV-50W voltammetric analyzer in a conventional three-electrode cell arrangement comprising a Pt coil counterelectrode, a Ag/Ag^+ (0.01 M, $TBAClO_4$ 0.1 M in CH_3CN) reference electrode, and a Pt working electrode (0.16 mm diameter). The spectra of oxidized poly-**11** were obtained in a electrochemical minicell mounted inside a quartz cuvette with an ITO glass modified with the polymer as the working electrode. ^1H NMR spectra were collected on a Varian Unit 500 MHz spectrometer and a JEOL GSX 270 MHz spectrometer with TMS ($\delta = 0.0$) as the reference. ^{13}C NMR data were recorded at 67.8 MHz with a JEOL GSX spectrometer. The DI-EI (70 eV) mass spectra were recorded with a Hitachi M80-B spectrometer. The SEM images were collected with a Jeol JSM-6700F microscope.

The *I–V* curves were collected with an Advantest R6245 2Channels Voltage Current Source Monitor interfaced to a microcomputer through a GPIB-SCSI board and NI-488.2 protocol. The data were acquired with a homemade procedure and IgorPro 4.0 (Wavemetrics) software. Triaxial cables were used to connect the molecular devices and the *I–V* monitor in order to minimize external noise. All measurements were carried out inside a vacuum chamber ($P < 2 \times 10^{-4}$ Pascal) equipped with a thermostat (±0.001 °C) and with liquid nitrogen as the coolant. The polymer was successfully prepared in situ between the gold nanogap electrodes (250 nm wide, gap width ~15 nm) by electropolymerization from a saturated solution of **11** in acetonitrile (0.1 M $TBAClO_4$). The nanogap electrodes were used as working and counterelectrodes, and a silver wire was employed as a pseudoreference electrode. The potentials were scanned 10 times in the 0–800 mV range. The procedure was repeated after the polarization had been reversed. The samples were then washed thoroughly with methanol and acetone and dried in vacuo. The details of the nanogap electrode fabrication were published elsewhere.[25]

3,8-Dibromo-1,10-phenanthroline (1): was prepared according to a previously reported method.[12]

3,8-Di(thiophen-2′,2″-yl)-1,10-phenanthroline (Dtphen, 2): Activated magnesium (0.672 g, 27.7 mmol) and dry THF (12 mL) were transferred to a round-bottom flask in a N_2 atmosphere. 2-Bromothiophene (1.22 mL, 12.6 mmol) was carefully added, and the mixture was left to react for 2 h at room temperature with constant stirring. A solution of **1** (1.52 g, 4.5 mmol) and $[NiCl_2(dppp)]$ (0.069 g, 0.127 mmol) in dry THF (15 mL) was prepared in a two-necked round-bottom flask connected to a fritted glass filter, and was then cooled to 0 °C in an ice/water bath. The previously prepared Grignard reagent was carefully added by means of a cannula, through the filter. The mixture was left to stand for 2 h at room temperature, and was then refluxed for 12 h. The reaction mixture was quenched with saturated NH_4Cl aqueous solution, extracted with $CHCl_3$, washed with a NaCl solution, and purified by column chromatography (silica gel, $CHCl_3$/*n*-hexane 1:1). A yellow crystalline product (1.45 g, 94 %) was obtained after removal of the solvent and drying in vacuo. ^1H NMR (270 MHz, $CDCl_3$): $\delta = 9.45$ (d, $J = 2.3$ Hz, 2H, phen), 8.34 (d, $J = 2.3$ Hz, 2H, phen), 7.82 (s, 2H, phen), 7.59 (dd, $J = 3.7$, 0.6 Hz, 2H, thiophenyl), 7.45 (dd, $J = 5.3$, 0.6 Hz, 2H, thiophenyl), 7.20 ppm (dd, $J = 5.3$, 3.7 Hz, 2H, thiophenyl); ^{13}C NMR (67.8 MHz, $CDCl_3$): $\delta =$ 148.12, 140.3, 131.6, 129.5, 128.6, 128.5, 127.2, 126.6, 125.0, 99.1 ppm; MS (DI-EI): *m/z*: 344 $[C_{20}H_{12}N_2S_2]^+$.

$[Ru(bpy)_2(OH_2)_2](NO_3)_2$: This complex was synthesized as a reactive intermediate in order to obtain the desired $[Ru(bpy)_2(L)]$ complexes (L = 3,8-bis(thiophene)-1,10-phenanthroline ligands) under mild conditions. The required amount was prepared immediately before use. Typically, $[Ru(bipy)_2Cl_2]\cdot H_2O$ (Aldrich, 0.1 g, 0.71 mmol) was suspended in a 1:1 methanol/water mixture (15 mL), heated to 70 °C, and the dissociated Cl^- ion precipitated by the addition of two equivalents of $Ag(NO)_3$ (Cica Reagents) in a N_2 atmosphere. The reaction mixture was stirred for 30 min, and the suspension was filtered through a thick Celite (Aldrich) bed. The clean solution was dried in the rotary evaporator to obtain the aqua complex as a dark solid, which was dissolved in DMF and reacted with the ligands **2**, **10**, and **12**, as described below.

Bis(2,2′-bipyridine)(3,8-(thiophen-2′,2″-yl)-1,10-phenanthroline)ruthenium(II) ($[Ru(bpy)_2(DTphen)](PF_6)_2$, 3): Compound **2** (0.24 g, 0.71 mmol) in $CHCl_3$ (10 mL) was reacted with an equivalent amount of $[Ru(bpy)_2(OH_2)_2](NO_3)_2$ in DMF (20 mL) for 10 min (60 °C). This intermediate was prepared from $[Ru(bpy)_2Cl_2]\cdot H_2O$ (0.34 g), as described above. The solvent was removed in the rotary evaporator. The solid was redissolved in DMF (15 mL), and the solution was added into an aqueous NH_4PF_6 solution (30 mL). The resultant brown solid was filtered, thoroughly washed with water, and dried in vacuo. Yield: 0.46 g (61 %); ^1H NMR (500 MHz, DMSO): $\delta = 9.05$ (d, $J = 1.8$ Hz, 2H, phen), 8.92 (d, $J = 8.2$ Hz, 2H, bpy), 8.83 (d, $J = 8.2$ Hz, 2H, bpy), 8.35 (s, 2H, phen), 8.29 (t, $J = 7.9$ Hz, 2H, bpy), 8.12 (t, $J = 7.9$ Hz, 2H, bpy), 8.03 (d, $J = 1.8$ Hz, 2H, phen), 7.96 (d, $J = 5.5$ Hz, 2H, bpy), 7.84 (d, $J = 5.8$ Hz, 2H, bpy), 7.78 (d, $J = 5.0$ Hz, 2H, thienyl), 7.66 (t, $J = 6.7$ Hz, 2H, bpy), 7.55 (d, $J = 3.6$ Hz, 2H, thienyl), 7.39 (t, $J = 6.7$ Hz, 2H, bpy), 7.24 ppm (dd, $J = 5.2$ and 3.6 Hz, 2H, thienyl); elemental analysis calcd (%) for $C_{40}H_{28}N_6S_2P_2F_{12}Ru$: C 45.85, H 2.69, N 8.02; found: C 45.07, H 2.90, N 7.90.

2,3,4,5-Tetrabromothiophene (4): Thiophene (0.3 mol) and $CHCl_3$ (12 mL) were transferred to a round-bottom flask and Br_2 (69 mL, 1.35 mol) was added dropwise into the vigorously stirred solution. The reaction mixture was kept at room temperature for 17 h and then refluxed for 2 h. After cooling to room temperature, a KOH solution (33 g) in ethanol (180 mL) was added. The mixture was refluxed for 4 h, poured into an ice/water mixture (400 mL), and extracted with $CHCl_3$. Colorless crystals of the desired product were obtained in 90 % yield after recrystallization from a $CHCl_3$/EtOH mixture. ^{13}C NMR ($CDCl_3$): $\delta =$ 116.94, 110.28 ppm; MS (EI): *m/z*: 400 ($C_4Br_4S^+$), 321, 240, 161.

3,4-Dibromothiophene (5): An acetic acid/water mixture (1:2, 180 mL) was transferred to a round-bottom flask, followed by the alternate addition of powdered zinc (60 g, 918 mmol) and **4** (113 g, 283 mmol) in small portions. The resultant mixture was kept at room temperature for 1 h and then refluxed for 3 h. The mixture was filtered through a celite bed and the product extracted with diethyl ether from the filtrate. The solution was dried with Na_2SO_4, the solvent was removed, and the residue then distilled under vacuum. A colorless liquid was obtained in 86 % yield. ^1H NMR (270 MHz, $CDCl_3$): $\delta = 7.29$ ppm (s, 2H); ^{13}C NMR ($CDCl_3$): $\delta = 123.73$, 113.88 ppm.

3,4-Dibutylthiophene (6): Magnesium (5.74 g, 236 mmol) was transferred to a three necked round-bottom flask and heated to 100 °C in a N_2 atmosphere. Dry diethyl ether (90 mL) and some I_2 were added, and the mixture was left to react for 10 min. *n*-Butylbromide (18.0 mL, 167.6 mmol) was carefully added to avoid excessive increase of temperature, and the

mixture was refluxed for an hour to obtain the corresponding Grignard reagent. Thiophene **5** (6.8 mL, 60.1 mmol) and [$NiCl_2$(dppp)] (1.02 g, 1.88 mmol) were transferred to a separate three-necked round-bottom flask connected to a sintered glass filter. After purging with N_2, dry diethyl ether (80 mL) was added and the Grignard reagent was carefully transferred through the filter. The reaction mixture was refluxed for 2 h, left to stand at room temperature for 12 h, and then quenched with 1 N HCl. It was then filtered through a celite bed and extracted with diethyl ether. The solvent was removed in a flash evaporator, and the residue was distilled. A colorless liquid was obtained in 85 % yield. ^{1}H NMR (270 MHz, $CDCl_3$): δ = 6.88 (s, 2H), 2.51 (t, J = 7.3 Hz, 4H), 1.66–1.52 (m, 4H), 1.47–1.36 (m, 4H), 0.95 ppm (t, J = 7.3 Hz, 4H); ^{13}C NMR (68 MHz, $CDCl_3$): δ = 142.04, 119.86, 31.82, 28.48, 22.65, 13.99 ppm; MS (DI-EI): m/z: 196 $[C_{12}H_{20}S]^+$; elemental analysis calcd (%) for $C_{12}H_{20}S$: C 73.40, H 10.27; found: C 73.15, H 10.07.

2,5-Dibromo-3,4-dibutylthiophene (7): Bromine (7.85 mL, 154.7 mmol) diluted in $CHCl_3$ (20 mL) was added to a solution obtained by mixing **6** (12.5 g, 63.7 mmol) and $CHCl_3$/acetic acid (1:2, 100 mL) in a round-bottom flask. The mixture was stirred overnight at room temperature and washed with water. The organic phase was washed five more times with water, the $CHCl_3$ was removed in a flash evaporator, and the residue was distilled in vacuo. A pale yellow liquid was obtained in 87 % yield. ^{1}H NMR (270 MHz, $CDCl_3$): δ = 2.52 (t, J = 7.6 Hz, 4H), 1.42 (m, 8H), 0.94 ppm (t, J = 7.2 Hz, 6H); ^{13}C NMR (68 MHz, $CDCl_3$): δ = 141.38, 107.81, 31.69, 28.65, 22.63, 13.87 ppm; MS (DI-EI): m/z: 354 $[C_{12}H_{18}Br_2S]^+$.

3,4-Dibutyl-2,2′:5′,2″-terthiophene (8): Magnesium (7.62 g) was transferred to a round-bottom flask and heated to 100 °C in a N_2 atmosphere. After the mixture was cooled down to room temperature, dry diethyl ether (140 mL) and some iodine were added, and the mixture was left to react for 10 minutes under magnetic stirring. 2-Bromothiophene (21.7 mL, 224 mmol, Aldrich) was then carefully added, and the mixture was refluxed for an hour to obtain the corresponding Grignard reagent. This was slowly added to a solution obtained by dissolving **7** (28.33 g, 80.0 mmol) and [$NiCl_2$(dppp)] (1.46 g, 2.70 mmol) in dry diethyl ether (150 mL). The mixture was refluxed for 4 h in a N_2 atmosphere. The reaction mixture was stirred for 12 h at room temperature, quenched with 1 N HCl, extracted with $CHCl_3$, and purified by silica column chromatography (*n*-hexane). A yellow liquid was obtained in 84 % yield. ^{1}H NMR (270 MHz, $CDCl_3$): δ = 7.27 (dd, J = 5.2, 1.1 Hz, 2H), 7.12 (dd, J = 3.7, 1.1 Hz, 2H), 7.04 (dd, J = 5.2, 3.7 Hz, 2H), 2.70 (t, J = 8.1 Hz, 4H), 1.51–1.41 (m, 8H), 0.94 ppm (t, J = 7.2 Hz, 6H); ^{13}C NMR (68 MHz, $CDCl_3$): δ = 139.99, 136.19, 129.80, 127.31, 125.81, 125.24, 32.90, 27.79, 22.98, 13.84 ppm; MS (DI-EI): m/z: 360 $[C_{20}H_{24}S_3]^+$; FT-IR (NaCl): $\tilde{\nu}$ = 2954, 2931, 2870, 2858, 1466, 845, 827, 692 cm^{-1}; elemental analysis calcd (%) for $C_{20}H_{24}S_3$: C 66.62, H 6.71; found: C 66.43, H 6.71.

5-Bromo-3′,4′-dibutyl-2,2′:5′,2″-terthiophene (9): A solution of NBS (1.24 g, 6.96 mmol) in acetic acid/$CHCl_3$ (1:1, 100 mL) was added dropwise to a solution of **8** (2.51 g, 6.96 mmol) in the same solvent (100 mL) cooled by an ice/water bath. The mixture was stirred overnight at room temperature, poured onto an aqueous NaCl solution (400 mL), and extracted with $CHCl_3$. The organic phase was washed five more times with distilled water. The solvent was removed in a flash evaporator, and the residue was purified by silica-gel column chromatography. A yellow liquid was obtained in 61 % yield. ^{1}H NMR (270 MHz, $CDCl_3$): δ = 7.29 (dd, J = 5.2, 1.2 Hz, 1H), 7.12 (dd, J = 3.7, 1.2 Hz, 1H), 7.05 (dd, J = 5.2, 3.7 Hz, 1H), 7.00 (d, J = 3.7 Hz, 1H), 6.86 (d, J = 3.7 Hz, 1H), 2.68 (t, J = 7.6 Hz, 2H), 2.65 (t, J = 7.9 Hz, 2H), 1.53–1.41 (br, 8H), 0.95 (t, J = 7.0 Hz, 3H), 0.94 ppm (t, J = 7.0 Hz, 3H); ^{13}C NMR (68 MHz, $CDCl_3$): δ = 140.49, 140.00, 137.73, 135.89, 130.36, 130.14, 128.79, 127.34, 126.02, 126.98, 125.45, 32.96, 32.87 27.79, 27.75, 22.96, 13.83 ppm; MS (DI-EI): m/z: 440 $[C_{20}H_{23}BrS_3]^+$; FT-IR (NaCl): $\tilde{\nu}$ = 2954, 2929, 2870, 2858, 1464, 970, 829, 790, 692 cm^{-1}; elemental analysis calcd (%) for $C_{20}H_{23}BrS_3$: C 54.66, H 5.27; found: C 54.77, H 5.28.

3,8-Bis(3′,4′-dibutyl-2,2′:5′,2″-terthiophen-5-yl)-1,10-phenanthroline (DBTT-phen, 10): A solution of terthiophene **9** (8.90 g, 20.25 mmol) in dry THF (15 mL) was added dropwise into a suspension of magnesium (0.77 g, 31.7 mmol, activated with I_2) in the same solvent (40 mL). The mixture was refluxed for 4 h in a N_2 atmosphere. A solution of **1** (2.59 g, 7.7 mmol) and [$NiCl_2$(dppp)] (0.43 g, 0.79 mmol) in dry THF (70 mL) was prepared, the Grignard reagent was added, and the mixture was refluxed for 10 h. The reaction was quenched with 1 M aqueous HCl, extracted with $CHCl_3$, washed with water, and purified by silica-gel column chromatography (60 % $CHCl_3$ in *n*-hexane) followed by recrystallization from a $CHCl_3$/*n*-hexane mixture. The product was obtained as yellow crystals in 40 % yield. ^{1}H NMR (270 MHz, $CDCl_3$): δ = 9.43 (d, J = 2.1 Hz, 2H), 8.30 (d, J = 2.1 Hz, 2H), 7.82 (s, 2H), 7.54 (d, J = 3.7 Hz, 2H), 7.33 (dd, J = 5.0, 1.2 Hz, 2H), 7.20 (d, J = 3.7 Hz, 2H), 7.17 (dd, J = 3.7, 1.2 Hz, 2H), 7.08 (dd, J = 5.0, 3.7 Hz, 2H), 2.79 (t, J = 9.3, 4H), 2.73 (t, J = 9.3 Hz, 4H), 1.59–1.47 (br, 16H), 1.01 (t, J = 7.2 Hz, 6H), 0.97 ppm (t, J = 7.2 Hz, 6H); ^{13}C NMR (68 MHz, $CDCl_3$): δ = 147.82, 144.81, 140.61, 140.29, 139.51, 137.74, 136.00, 130.98, 130.45, 129.37, 129.24, 128.45, 127.40, 127.20, 126.84, 125.99, 125.48, 125.27, 32.90, 32.82, 27.99, 27.82, 23.05, 22.99, 13.88, 13.85 ppm; MS (FAB): m/z: 897.3 $[C_{52}H_{52}N_2S_6]^+$; FT-IR (KBr): $\tilde{\nu}$ = 2954, 2931, 1558, 1521, 1473 cm^{-1}; elemental analysis calcd (%) for $C_{52}H_{54}N_2S_6O$: C 68.23, H 5.95, N 3.06; found: C 68.54, H 5.81, N 2.83.

Bis(2,2′-bipyridyl)(3,8-bis(3′,4′-dibutyl-2,2′:5′,2″-terthiophen-5-yl)-1,10-phenanthroline)ruthenium(II), $[Ru(bipy)_2(10)](PF_6)_2$ (11): The ruthenium complex was obtained by the reaction of compound **11** (50 mg, 0.056 mmol/5 mL $CHCl_3$) and an equivalent amount of $[Ru(bpy)_2(OH_2)_2](NO_3)_2$ in DMF (10 mL), as described above. This mixture was concentrated in a flash evaporator and added to an aqueous NH_4PF_6 solution. The precipitate was collected, washed with water, and dried in vacuo. A dark-red solid was obtained in 71 % yield (59 mg). ^{1}H NMR (500 MHz, [D$_6$]DMSO): δ = 9.04 (d, J = 1.7 Hz, 2H, phen), 8.90 (d, J = 8.3 Hz, 2H, bpy), 8.84 (d, J = 8.3 Hz, 2H, bpy), 8.35 (s, 2H, phen), 8.28 (t, J = 7.9, 2H, bpy), 8.13 (t, J = 7.9 Hz, 2H, bpy), 8.07 (d, J = 1.9 Hz, 2H, phen), 7.94 (d, J = 5.1 Hz, 2H, bpy), 7.86 (d, J = 5.1 Hz, 2H, bpy), 7.68 (d, J = 5.1, 2H, thienyl), 7.65 (t, J = 6.7, 2H, bpy), 7.54 (d, J = 3.9 Hz, 2H, thienyl), 7.41 (t, J = 6.7, 2H, bpy), 7.34 (d, J = 3.9 Hz, 2H, thienyl), 7.25 (d, J = 3.5 Hz, 2H, thienyl), 7.18 (dd, J = 5.1 and 3.5 Hz, 2H, thienyl), 2.70 (br, 8H, butyl), 1.49 (br, 8H, butyl), 1.41 (br, 8H, butyl), 0.95 ppm (br, 12H, butyl); MS (FAB): m/z: 1600.3 $[C_{72}H_{68}N_6RuS_6P_2F_{12}]^+$, 1455.3 $[C_{72}H_{68}N_6RuS_6PF_6]^+$; FT-IR (KBr): $\tilde{\nu}$ = 630, 2343, 2329 cm^{-1}; elemental analysis calcd (%) for $C_{72}H_{68}N_6S_6P_2F_{12}Ru$: C 54.02, H 4.28, N 5.25; found: C 54.30, H 4.26, N 5.28.

3,8-Bis(3′,4′-dibutyl-5″-thiocyanato-2,2′:5′,2″-terthiophen-5-yl)-1,10-phenanthroline (12): A solution of compound **10** (1.35 g) in $CHCl_3$ (60 mL) was added to a mixture of KSCN (1.35 g, 1.5 mmol), Br_2 (4.6 mL, 89.8 mmol), and $CHCl_3$ (15 mL) at −70 °C. This mixture was stirred for 4 h at room temperature, quenched with water, extracted with $CHCl_3$, and purified by silica-gel column chromatography ($CHCl_3$). A yellow crystalline product was obtained (94 % yield) after recrystallization from $CHCl_3$/*n*-hexane. ^{1}H NMR (270 MHz, $CDCl_3$): δ = 9.44 (d, J = 2.1 Hz, 2H), 8.34 (d, J = 2.1 Hz, 2H), 7.86 (s, 2H), 7.57 (d, J = 3.7 Hz, 2H), 7.41 (d, J = 4.0 Hz, 2H), 7.24 (d, J = 3.7 Hz, 2H), 7.12 (d, J = 4.0 Hz, 2H), 2.77 (m, 8H), 1.56–1.25 (br, 16H), 1.01 (t, J = 7.0 Hz, 6H), 0.99 ppm (t, J = 7.0 Hz, 6H); ^{13}C NMR (68 MHz, $CDCl_3$): δ = 147.77, 144.49, 141.88, 140.89, 140.09, 138.10, 137.03, 131.15, 131.06, 128.59, 127.36, 127.27, 126.48, 125.39, 116.39, 110.23, 32.81, 27.94, 23.02, 22.98, 13.86, 13.83 ppm; MS (FAB): m/z: 1011.3 $[C_{54}H_{50}N_4S_8]^+$; FT-IR (KBr): $\tilde{\nu}$ = 2954, 2156, 1558, 1506, 1419, 796 cm^{-1}; elemental analysis calcd (%) for $C_{54}H_{50}N_4S_8$: C 64.12, H 4.98, N 5.54; found: C 64.19, H 5.02, N 5.52.

Bis(2,2′-bipyridyl)(3,8-bis(3′,4′-dibutyl-5″-thiocyanato-2,2′:5′,2″-terthiophen-5-yl)-1,10-phenanthroline)ruthenium(II) ($[Ru(bipy)_2(12)](PF_6)_2$, 13): This ruthenium complex was obtained by the reaction of compound **12** (114 mg, 0.11 mmol) in $CHCl_3$ (5 mL) with an equivalent amount of $[Ru(bpy)_2(OH_2)_2](NO_3)_2$ dissolved in DMF (10 mL). The product, precipitated as the PF_6^- salt, was recrystallized as a red-orange solid by dropwise addition of methanol into a concentrated acetone solution. Yield: 153 mg (84 %); ^{1}H NMR (500 MHz, [D$_6$]DMSO): δ = 9.06 (d, J = 2.0 Hz, 2H, phen), 8.90 (d, J = 8.5 Hz, 2H, bpy), 8.83 (d, J = 8.0 Hz, 2H, bpy), 8.36 (s, 2H, phen), 8.28 (t, J = 7.5 Hz, 2H, bpy), 8.12 (t, J = 8.5 Hz, 2H, bpy), 8.08 (d, J = 2.0 Hz, 2H, phen), 7.93 (d, J = 5.5 Hz, 2H, bpy), 7.85 (d, J = 5.5 Hz, 2H, bpy), 7.69 (d, J = 4.5 Hz, 2H, thienyl), 7.65 (t, J = 7.0 Hz, 2H, bpy), 7.56 (d, J = 3.5 Hz, 2H, thienyl), 7.40 (t, J = 6.5 Hz, 2H, bpy), 7.39 (d, J = 4.5 Hz, 2H, thienyl), 7.31 (d, J = 4.0 Hz, 2H, thienyl), 2.72 (br, 8H, butyl), 1.49 (br, 8H, butyl), 1.40 (br, 8H, butyl), 0.93 (br, 12H, butyl); elemental analysis calcd (%) for

$C_{76}H_{72}F_{12}N_8P_2RuS_8$ C 52.31, H 4.16, N 6.42; found: C 51.49, H 4.25, N 6.38.

Acknowledgement

This work was supported by a Grant-in-Aid for Scientific Research (No. 15201028 and No. 14654135) from the Ministry of Culture, Education, Science Sports, and Technology of Japan.

[1] a) C. Joachim, J. K. Gimzewski, A. Aviram, *Nature* **2000**, *408*, 541–548; b) *Molecular Electronics* (Eds.: M. A. Reed, T. Lee), American Scientific Publishers, Stevenson Ranch, CA, **2003**.

[2] a) P. Kovacic, M. B. Jones, *Chem. Rev.* **1987**, *87*, 357–379; b) J. Roncali, *Chem. Rev.* **1997**, *97*, 173–205; c) T. Yamamoto, Y. Yoneda, K. Kizu, **1995**, *16*, 549–556; d) N. Aratani, A. Tsuda, A. Osuka, *Synlett* **2001**, *11*, 1663–1674; e) A. Osuka, N. Tanabe, S. Nakajima, K. Maruyama, *J. Chem. Soc. Perkin Trans. 2* **1996**, *2*, 199–203.

[3] a) J. Park, A. N. Pasupathy, J. I. Goldsmith, C. Chang, Y. Yaish, J. R. Petta, M. Rinkoski, J. P. Sethna, H. D. Abrunã, P. L. McEuen, D. C. Ralph, *Nature* **2002**, *417*, 722–725; b) W. Liang, M. P. Shores, M. Bockrath, J. R. Long, H. Park, *Nature* **2002**, *417*, 725–729.

[4] a) S. Kubatkin, A. Danilov, M. Hjort, J. Cornil, J.-L. Bredas, N. Stuhr-Hansen, P. Hedegard, T. Bjørnholm, *Nature* **2003**, *425*, 698–701; b) J. Chen, T. Lee, J. Su, W. Wang, M. A. Reed, M. A. Rawlett, M. Kozaki, Y. Yao, R. C. Jagessar, S. M. Dirk, D. S. Grubisha, D. W. Bennett in *Molecular Nanoelectronics: Molecular Electronic Devices* (Eds.: M. A. Reed, T. Lee), American Scientific Publishers, Stevenson Ranch, CA, **2003**, pp. 39–114; c) M. L. Chabinyc, X. Chen, R. E. Holmlin, H. Jacobs, H. Skulason, C. D. Frisbie, V. Mujica, M. A. Ratner, M. A. Rampi, G. M. Whitesides, *J. Am. Chem. Soc.* **2002**, *124*, 11730–11736; d) C. P. Collier, J. O. Jeppesen, Y. Luo, J. Perkins, E. W. Wong, J. R. Heath, J. F. Stoddart, *J. Am. Chem. Soc.* **2001**, *123*, 12632–12641.

[5] A. Nitzan, M. A. Ratner, *Science* **2003**, *300*, 1384–1389.

[6] T. Ogawa, K. Kobayashi, G. Masuda, T. Takase, S. Maeda, *Thin Solid Films* **2001**, *393*, 374–378.

[7] L. Tan, M. D. Curtis, A. H. Francis, *Macromolecules* **2002**, *35*, 4628–4635.

[8] a) H. Sirringhaus, N. Tessler, R. H. Friend, *Science* **1998**, *280*, 1741–1744; b) T. Yamamoto, H. Suganuma, T. Maruyama, T. Inoue, Y. Muramatsu, M. Arai, D. Komarudin, N. Ooba, S. Tomaru, S. Sasaki, K. Kubota, *Chem. Mater.* **1997**, *9*, 1217–1225.

[9] Y. Zhu, M. O. Wolf, *J. Am. Chem. Soc.* **2000**, *122*, 10121–10125.

[10] B. J. MacLean, P. G. Pickup, *J. Mater. Chem.* **2001**, *11*, 1357–1363.

[11] S. S. Zhu, R. P. Kingsborough, T. M. Swager, *J. Mater. Chem.* **1999**, *9*, 2123–2131.

[12] Y. Saitoh, T. Yamamoto, *Chem. Lett.* **1995**, 785–786.

[13] a) B. L. Lee, T. Yamamoto, *Macromolecules* **1999**, *32*, 1375–1382; b) T. Yamamoto, Z. H. Zhou, T. Kanbara, M. Shimura, K. Kizu, T. Maruyama, Y. Nakamura, T. Fukuda, B. L. Lee, N. Ooba, S. Tomaru, T. Kurihara, T. Kaino, K. Kubota, S. Sasaki, *J. Am. Chem. Soc.* **1996**, *118*, 10389–10399.

[14] a) T. Yamamoto, Z. H. Zhou, T. Maruyama, T. Kanbara, *Synth. Met.* **1993**, *55*, 1209–1213; b) Z. H. Zhou, T. Maruyama, T. Kanbara, T. Ikeda, K. Ichimura, T. Yamamoto, K. Tokuda, *J. Chem. Soc. Chem. Commun.* **1991**, 1210–1212.

[15] T. M. Pappenfus, K. R. Mann, *Inorg. Chem.* **2001**, *40*, 6301–6307.

[16] Y. Yu, E. Gunic, B. Zinger, L. L. Miller, *J. Am. Chem. Soc.* **1996**, *118*, 1013–1018; L. L. Miller, Y. Yu, *J. Org. Chem.* **1995**, *60*, 6813–6819.

[17] J. Roncali, *Chem. Rev.* **1992**, *92*, 711–738.

[18] A. Juris, V. Balzani, F. Barigelletti, S. Campagna, P. Belser, A. Vonzelewsky, *Coord. Chem. Rev.* **1988**, *84*, 85–277.

[19] K. A. Walters, L. Trouillet, S. Guillerez, F. S. Schanze, *Inorg. Chem.* **2000**, *39*, 5496–5509.

[20] L. Trouillet, A. De Nicola, S. Guillerez, *Chem. Mater.* **2000**, *12*, 1611–1621.

[21] a) M. Maggini, D. M. Guldi, S. Mondini, G. Scorrano, F. Paolucci, P. Ceroni, S. Roffia, *Chem. Eur. J.* **1998**, *4*, 1992–2000; b) S. Roffia, M. Marcaccio, C. Paradisi, F. Paolucci, V. Balzani, G. Denti, S. Serroni, S. Campagna, *Inorg. Chem.* **1993**, *32*, 3003–3009.

[22] S. Encinas, L. Flamigni, F. Barigelletti, E. C. Constable, C. E. Housecroft, E. R. Schofield, E. Figgemeier, D. Fenske, M. Neuburger, J. G. Vos, M. Zehnder, *Chem. Eur. J.* **2002**, *8*, 137–150.

[23] a) M. C. Hodgson, A. K. Burrell, P. D. W. Boyd, P. J. Brothers, C. E. F. Rickard, *J. Porphyrins Phthalocyanines* **2002**, *6*, 737–747; b) H. E. Toma, K. Araki, *Coord. Chem. Rev.* **2000**, *196*, 307–329; c) H. E. Toma, K. Araki, A. D. P. Alexiou, S. Nikolaou, S. Dovidauskas, *Coord. Chem. Rev.* **2001**, *219*, 187–234; d) K. Araki, P. Losco, F. M. Engelmann, H. Winnischofer, H. E. Toma, *J. Photochem. Photobiol. A* **2001**, *142*, 25–30; e) S. W. Rhee, Y. H. Na, Y. Do, J. Kim, *Inorg. Chim. Acta* **2000**, *309*, 49–56; f) J. L. Sessler, V. L. Capuano, A. K. Burrell, *Inorg. Chim. Acta* **1993**, *204*, 93–101.

[24] a) J. F. Endicott, H. B. Schlegel, M. J. Uddin, D. S. Seniveratne, *Coord. Chem. Rev.* **2002**, *229*, 95–106; b) M. Marcaccio, F. Paolucci, C. Paradisi, M. Carano, S. Roffia, C. Fontanesi, L. J. Yellowlees, S. Serroni, S. Campagna, V. Balzani, *J. Electroanal. Chem.* **2002**, *532*, 99–112; c) M. Marcaccio, F. Paolucci, C. Paradisi, S. Roffia, C. Fontanesi, L. J. Yellowlees, S. Serroni, S. Campagna, C. Denti, V. Balzani, *J. Am. Chem. Soc.* **1999**, *121*, 10081–10091; d) R. C. Rocha, K. Araki, H. E. Toma, *Inorg. Chim. Acta* **1999**, *285*, 197–202.

[25] K. Araki, H. Endo, H. Tanaka, T. Ogawa, *Jap. J. Appl. Phys.* **2004**, *43 (5A)*, L634–L636.

[26] P. Belser, A. V. Zelewsky, *Helv. Chim. Acta* **1980**, *63*, 1675–1702.

[27] H. Chen, J. Q. Lu, J. Wu, R. Note, H. Mizuseki, Y. Kawazoe, *Phys. Rev. B* **2003**, *67*, 4.

Received: January 20, 2004

Published online: April 29, 2004

